An approach for modeling non-ageing linear viscoelastic composites with general periodicity

O.L. Cruz-González, D. Guinovart-Sanjuán, R. Rodríguez-Ramos, J. Bravo-Castillero, R. Guinovart-Díaz, J. Merodio, R. Penta, José A. Otero, Serge Dumont, Frédéric Lebon, et al.

An approach for modeling non-ageing linear viscoelastic composites with general periodicity

O.L. Cruz-González[a], D. Guinovart-Sanjuán[b], R. Rodríguez-Ramos[c,*], J. Bravo-Castillero[d], R. Guinovart-Díaz[c], J. Merodio[e], R. Penta[f], José A. Otero[g], S. Dumont[h], F. Lebon[a], F.J. Sabina[d]

[a] *Aix-Marseille Univ., CNRS, Centrale Marseille, LMA, 4 Impasse Nikola Tesla, CS 40006, 13453 Marseille Cedex 13, France*
[b] *Department of Mathematics, University of Central Florida, 4393 Andromeda Loop N, Orlando, FL 32816, USA*
[c] *Facultad de Matemática y Computación, Universidad de La Habana, San Lázaro y L, Vedado, La Habana CP 10400, Cuba*
[d] *Instituto de Investigaciones en Matemáticas Aplicadas y en Sistemas (IIMAS). Universidad Nacional Autónoma de México, Apartado Postal 20-126, Alcaldía de Álvaro Obregón, 01000 CDMX, Mexico*
[e] *Departamento de Mecánica de los Medios Continuos y T. Estructuras, E.T.S. de Caminos, Canales y Puertos, Universidad Politécnica de Madrid, C.P. 28040, Spain*
[f] *School of Mathematics and Statistics, Mathematics and Statistics Building, University of Glasgow, University Place, Glasgow G12 8QQ, UK*
[g] *Tecnológico de Monterrey, Escuela de Ingeniería y Ciencias, Atizapán de Zaragoza, Estado de México, Mexico*
[h] *Universîté de Nîmes, Institut de Mathématiques Alexander Grothendieck, CNRS, UMR 5149, CC.051, Pl. E. Bataillon, 34 095 Montpellier Cedex 5, France*

The present work deals with the modeling of non-ageing linear viscoelastic composite materials and quasi-periodic microstructure. The stratified functions and the curvilinear coordinates play an important role in the design of different geometrical shapes. The main objective focuses on the application of two-scales Asymptotic Homogenization Method (AHM) to obtain the overall behavior of the viscoelastic composite materials. Although the whole process is based on the analysis of laminated configurations, a multi-step homogenization scheme to estimate the effective properties of a structure reinforced with long rectangular fibers and wavy effects is used. The associated local problems, the homogenized problem and the analytical expressions for the effective coefficients are obtained by using the correspondence principle and the Laplace-Carson transform. Also, the interconnection between the effective relaxation modulus and the effective creep compliance is performed. Finally, the inversion to the original temporal space is calculated. Some comparisons between the proposed approach and Finite Elements Method (FEM) results are displayed.

1. Introduction

Nowadays, the performance of mechanical properties as weight, heat resistance, corrosion, among others are optimized thanks to the use of composite materials. Besides, another advantage is the possibility of individually controlling each component (or phase) and its corresponding distribution in the microstructure (see Maghous and Creus 2003 [1]).

The modeling of composite materials requires the development of micromechanics techniques to predict the general (or effective) properties of the heterogeneous structure from the properties, density, proportion and arrangement of its constituents. An excellent review on these methods can be found in Kalamkarov et al. 2009 [2] and Sevostianov and Giraud 2013 [3]. On the other hand, the recent growth of polymeric matrix composites in the aerospace, aeronautical and automobile industry, as well as in bioengineering applications, due to their high strength-to-weight and moduli-to-weight ratios, is an evidence of the usefulness of viscoelastic materials in the design of durable and sustainable structural components. Viscoelastic materials usually establish both instant (elastic) and time-dependent (viscous) behavior, stimulating the investigations in composites and the study of creep and relaxation characteristics.

Some authors have used different schemes to calculate the effective properties of viscoelastic composite materials, for example, Maxwell's homogenization is used in Sevostianov et al. 2015 [4], self-consistent generalized scheme is applied in Honorio et al. 2017 [5] and Mori–Tanaka homogenization is studied in Schöneich et al. 2017 [6].

The two-scales Asymptotic Homogenization Method (AHM) is proposed in this research. The theoretical aspects and the fact that the solution of the heterogeneous problems converges weaker to the solution of the homogeneous problems, when the small parameter which describes the microstructure tends to zero, are rigorously developed by

* Corresponding author.
E-mail address: reinaldo@matcom.uh.cu (R. Rodríguez-Ramos).

Bensoussan et al. 1978 [7], Sanchez-Palencia 1980 [8], Pobedria 1984 [9], Bakhvalov & Panasenko 1989 [10], Oleinik et al. 1992 [11] and Cioranescu & Donato 1999 [12]. The AHM is applied to problems with rapidly oscillating parameters, where the structures are strongly heterogeneous. It is a direct method because it allows, through the solution of the local problems, directly obtain the sought effective properties. Many papers have exhibited their potentialities for elastic (see Ramírez-Torres et al. 2018 [13]), thermo-elastic (see Chatzigeorgiou et al. 2012 [14]) and piezoelectric materials (see Rodríguez-Ramos et al. 2014 [15]). Moreover, it gives suitable solution in the case of fibrous viscoelastic composites (see Berger et al. 2018 [16] and Li et al. 2019 [17]).

Actually, the investigation of the effective properties of non-ageing viscoelastic composites are mainly based on the correspondence principle and the Laplace transform (see Hashin 1965 [18], 1970a [19], 1970b [20], Mandel 1966 [21], Christensen 1969 [22], Lahellec & Suquet 2007 [23]). The procedure, see for example Pasa Dutra et al. 2010 [24] and To et al. 2017 [25], consists into the change of the convolution constitutive law which describes the non-ageing viscoelastic behavior, into a fictitious elastic one in the Laplace domain. Then, the inversion of Laplace transform is considered to derive the effective behavior in the time domain.

Many heterogeneous structures are characterized by more general periodic functions (see Tsalis et al. 2012 [26], Tsalis et al. 2013 [27]). These functions, called *of stratification*, describe the microstructure of the composite material. The concept was introduced by Bensoussan et al. 1978 [7] and developed by Briane 1993 [28]. These ideas are related to homogenization problems of shell-type structures of widely technological interest (nano–hulls, fibre-reinforced polymers (FRP), civil engineering structures repair, modeling of human heart tissue).

The present work deals with the study of a non-ageing linear viscoelastic heterogeneous problem, which involves concepts of generalized periodicity and curvilinear coordinates. The proposed solutions are based on the application of the AHM, where the formulas for the local problems, the homogenized problem and the effective coefficients are given analytically. The aforementioned results are obtained in the Laplace-Carson space and a numerical algorithm is developed for computing the effective properties of the composites into the original temporal space. Considering the use of stratified functions, some laminated structures are studied and their effective properties are calculated. Also, a two-steps homogenization scheme to predict the effective properties of a viscoelastic composite material reinforced with long rectangular fibers and wavy effects is applied. An interconversion procedure between the effective relaxation modulus and the effective creep compliance is developed. It allows to obtain information about both properties using the same model. A numerical algorithm using FEM is developed and the comparisons are displayed.

2. Viscoelastic problem for curvilinear structures

A linear viscoelastic heterogeneous material which occupies a region Ω in $\mathbb{R}^3$ and possesses a quasi-periodic microstructure is considered. The concept of quasi-periodicity or generalized periodicity has been used by some authors such as Guinovart-Sanjuán et al. (2016) [29] and Tsalis et al. (2012) [26]). It is equivalent to affirm that exist a curvilinear coordinate system $\boldsymbol{x}(x_i)$ and a function $\boldsymbol{\varphi}$: $\mathbb{R}^3 \to \mathbb{R}^3$ such that the operator $\boldsymbol{\sigma} = \mathscr{F}\left(\boldsymbol{\varepsilon}; \boldsymbol{x}, \frac{\boldsymbol{\varphi}(\boldsymbol{x})}{\epsilon}, t\right)$, which relates the stress tensor $\boldsymbol{\sigma}(\sigma^{ij})$ and the strain tensor $\boldsymbol{\varepsilon}$ (ε_{kl}), is regular in $\boldsymbol{x}$ and $\mathbf{Y}$-periodic in $\boldsymbol{y}$, where $\boldsymbol{y} = \frac{\boldsymbol{\varphi}(\boldsymbol{x})}{\epsilon}$ and $\mathbf{Y}$ is the unit cell.

The equilibrium equation under the action of external force field is written as

$$\operatorname{div} \boldsymbol{\sigma}(\boldsymbol{x}, t) + \boldsymbol{f}(\boldsymbol{x}, t) = \mathbf{0}, \quad \text{in} \quad \Omega \times \mathbb{R}. \tag{1}$$

The corresponding boundary conditions associated to (1) are

$$\boldsymbol{u}(\boldsymbol{x}, t) = \boldsymbol{u}^0, \quad \text{on} \quad \Sigma_1 \times \mathbb{R}, \tag{2}$$

$$\boldsymbol{\sigma}(\boldsymbol{x}, t)\cdot\boldsymbol{n} = \boldsymbol{s}_0, \quad \text{on} \quad \Sigma_2 \times \mathbb{R}, \tag{3}$$

and the initial condition is taken as follows

$$\boldsymbol{u}(\boldsymbol{x}, t) = \mathbf{0}, \quad \text{in} \quad \Omega \times \{0\}, \tag{4}$$

where $\Sigma_1 \cup \Sigma_2 = \partial\Sigma$ and $\Sigma_1 \cap \Sigma_2 = \varnothing$.

Here, the external force field, surface force field, displacement field and outer unit normal to the boundary $\partial\Sigma$ of Ω are denoted by $\boldsymbol{f}(f^i)$, $\boldsymbol{s}_0(s_0^i)$, $\boldsymbol{u}^0(u_i^0)$ and $\boldsymbol{n}(n_i)$, respectively.

Taking into account the summation convention, the equilibrium Eq. (1) for a curvilinear coordinate system $\boldsymbol{x}$ can be written

$$\sigma^{ij}\|_j(\boldsymbol{x}, t) + f^i(\boldsymbol{x}, t) = \sigma^{ij}_{\ j}(\boldsymbol{x}, t) + \Gamma^i_{jk}(\boldsymbol{x})\sigma^{kj}(\boldsymbol{x}, t) + \Gamma^j_{jk}(\boldsymbol{x})\sigma^{ik}(\boldsymbol{x}, t) + f^i(\boldsymbol{x}, t) = 0, \tag{5}$$

where $\{\cdot\}\|_j$ denotes the covariant derivative, $\{\cdot\}_{,j} = \frac{\partial}{\partial x_j}\{\cdot\}$ represents the derivative in relation to the global curvilinear coordinate $\boldsymbol{x}$ and Γ^i_{jk} denotes the Christoffel symbols (see Taber 2004 [30]).

The constitutive law which relates the stress and strain fields (see Christensen 1982 [31] and Pipkin 1986 [32]) is proposed

$$\boldsymbol{\sigma}(\boldsymbol{x}, t) = \int_0^t \boldsymbol{R}\left(\boldsymbol{x}, \frac{\boldsymbol{\varphi}(\boldsymbol{x})}{\epsilon}, t - \tau\right) : \frac{\partial \boldsymbol{\varepsilon}(\boldsymbol{u}(\boldsymbol{x}, \tau))}{\partial \tau} d\tau, \tag{6}$$

where $\boldsymbol{R}$ (R^{ijkl}) represents a fourth rank tensor denominated relaxation modulus. The following relationship is satisfied for small displacements

$$\varepsilon_{kl}(\boldsymbol{u}(\boldsymbol{x}, t)) = \frac{1}{2}(u_k\|_l(\boldsymbol{x}, t) + u_l\|_k(\boldsymbol{x}, t)). \tag{7}$$

The statement of the constitutive law (6) corresponds to the special form of non-ageing linear viscoelastic materials (see Maghous and Creus 2003 [1]). The viscoelastic problem can be transformed into an elastic problem using the Laplace-Carson transform. This is known as the correspondence principle.

The Laplace-Carson transform is defined by

$$L_C[\boldsymbol{g}(\boldsymbol{x}, t)] = \widetilde{\boldsymbol{g}}(\boldsymbol{x}, p) = p\int_0^\infty e^{-pt}\boldsymbol{g}(\boldsymbol{x}, t)dt,$$

and the functions with the symbol $(\widetilde{\ })$ depending on the parameter p denote the Laplace-Carson space.

Applying the Laplace-Carson transform to (6) and considering the convolution theorem (see Appendix B in Christensen 1982 [31]) the constitutive law is written by components

$$\widetilde{\sigma}^{ij}(\boldsymbol{x}, p) = \widetilde{R}^{ijkl}\left(\boldsymbol{x}, \frac{\boldsymbol{\varphi}(\boldsymbol{x})}{\epsilon}, p\right)\varepsilon_{kl}(\widetilde{\boldsymbol{u}}(\boldsymbol{x}, p)). \tag{8}$$

Including the symmetry properties $R^{ijkl} = R^{jikl} = R^{ijlk} = R^{klij}$ for the relaxation modulus, Eq. (8) is transformed into

$$\widetilde{\sigma}^{ij}(\boldsymbol{x}, p) = \widetilde{R}^{ijkl}\left(\boldsymbol{x}, \frac{\boldsymbol{\varphi}(\boldsymbol{x})}{\epsilon}, p\right)\widetilde{u}_k\Big\|_l(\boldsymbol{x}, p). \tag{9}$$

Finally, substituting (9) into (5) and using (2)–(4), the mathematical statement for quasi-static viscoelastic heterogeneous problems in the Laplace-Carson space is written

$$\left(\widetilde{R}^{ijmn}\left(\boldsymbol{x}, \tfrac{\boldsymbol{\varphi}(\boldsymbol{x})}{\epsilon}, p\right)(\widetilde{u}_{m,n}(\boldsymbol{x}, p) - \Gamma^r_{mn}(\boldsymbol{x})\widetilde{u}_r(\boldsymbol{x}, p))\right)_{,j} + \left(\Gamma^i_{jk}(\boldsymbol{x})\widetilde{R}^{kjmn}\left(\boldsymbol{x}, \tfrac{\boldsymbol{\varphi}(\boldsymbol{x})}{\epsilon}, p\right) + \Gamma^j_{jk}(\boldsymbol{x})\widetilde{R}^{ikmn}\left(\boldsymbol{x}, \tfrac{\boldsymbol{\varphi}(\boldsymbol{x})}{\epsilon}, p\right)\right) \cdot (\widetilde{u}_{m,n}(\boldsymbol{x}, p) - \Gamma^r_{mn}(\boldsymbol{x})\widetilde{u}_r(\boldsymbol{x}, p)) + \widetilde{f}^{\,i}(\boldsymbol{x}, p) = 0, \tag{10}$$

with boundary conditions

$$\widetilde{u}_i(\boldsymbol{x}, p) = u_i^0 \text{ on } \Sigma_1 \times [0, +\infty), \tag{11}$$

$$\left(\widetilde{R}^{ijmn}\left(\boldsymbol{x},\frac{\boldsymbol{\varphi}(\boldsymbol{x})}{\epsilon},p\right)(\widetilde{u}_{m,n}(\boldsymbol{x},p)-\Gamma^{r}_{mn}(\boldsymbol{x})\widetilde{u}_{r}(\boldsymbol{x},p))\right)n_j = s^{i}_{0} \text{ on } \Sigma_2\times[0,+\infty), \tag{12}$$

and initial conditions,

$$\widetilde{u}_i(\boldsymbol{x},0)=0 \text{ in } \Omega\times\{0\}. \tag{13}$$

Some additional remarks in order to ensure the existence of unique weak solution of the problem (see Bakhvalov and Panasenko 1989 [10], Persson et al. 1993 [33], Tsalis et al. 2012 [26]) are given as follows:

1. $\boldsymbol{x}$ and $\boldsymbol{y}$ are named global and local curvilinear coordinate, respectively. The function $\boldsymbol{\varphi}$: $\Omega\longrightarrow\mathbb{R}^3$ characterizes the viscoelastic curvilinear structure and satisfies $\boldsymbol{\varphi}\in\ C^{\infty}(\Omega)$. The parameter ϵ is the fine mesh size of the unit cell structure $\mathbf{Y}\subset\mathbb{R}^3$ and $\epsilon = V_{\mathbf{Y}}/V_{\Omega}\ll 1$, where $V_{\mathbf{Y}}$ denotes the volumen of $\mathbf{Y}$ and V_{Ω} the volumen of Ω.
2. The relaxation modulus is assumed $\boldsymbol{R}(\boldsymbol{x},\boldsymbol{y},t)\in L^{\infty}(\Omega\times\mathbb{R})$. Moreover, $\boldsymbol{R}_{\epsilon}\left(\boldsymbol{x},\frac{\boldsymbol{\varphi}(\boldsymbol{x})}{\epsilon},t\right)=\boldsymbol{R}(\boldsymbol{x},\boldsymbol{y},t)$ is regular in $\boldsymbol{x}$ and $\mathbf{Y}$-periodic in $\boldsymbol{y}$.
3. $\boldsymbol{R}(\boldsymbol{x},\boldsymbol{y},t)$ is positively definite, i.e., $R^{ijkl}\xi^{ij}\xi^{kl}\geqslant\lambda\xi^{ij}\xi^{kl}$ for all symmetric real valued tensors ξ^{ij} and some positive constant λ.
4. $\exists\ \alpha,\beta,t_0$ such that $0<\alpha\leqslant\boldsymbol{R}(\boldsymbol{x},\boldsymbol{y},t_0)\leqslant\beta<+\infty\quad\forall\,\boldsymbol{x}\in\Omega,\ \forall\,\boldsymbol{y}\in\mathbb{R}^3(\epsilon\to 0)$.
5. $\boldsymbol{f}(\boldsymbol{x},t)\in L^2(\Omega\times\mathbb{R})$.

3. Two-scale asymptotic homogenization method

In this section, AHM is used to solve the heterogeneous problem (10)–(13). The solution is proposed as follows,

$$\widetilde{u}(\boldsymbol{x},\epsilon,p)=\sum_{a=0}^{+\infty}\epsilon^{a}\ \widetilde{\boldsymbol{u}}^{(a)}\left(\boldsymbol{x},\frac{\boldsymbol{\varphi}(\boldsymbol{x})}{\epsilon},p\right), \tag{14}$$

where $\widetilde{\boldsymbol{u}}^{(a)}$ ($\widetilde{u}_i^{(a)}$) is regular in $\boldsymbol{x}$ and $\mathbf{Y}$-periodic related to the variable $\boldsymbol{y}$ $\forall\ a\in\mathbb{N},\ \forall\,\boldsymbol{x}\in\Omega,\ \forall\ p\in[0,+\infty)$ and $\widetilde{\boldsymbol{u}}^{(a)}\left(\boldsymbol{x},\frac{\boldsymbol{\varphi}(\boldsymbol{x})}{\epsilon},p\right)\in C^{\infty}(\Omega\times[0,+\infty))$.

The main objective is to build (14) as *a formal asymptotic solution* for the problem (10)–(13) such that the approximation be of the order $\mathbf{O}(\epsilon)$. This truncation is enough to ensure that the solution of the homogenized problem converge weaker to the solution of heterogeneous problem when $\epsilon\to 0$. (see Bakhvalov and Panasenko 1989 [10]).

According to the chain rule, the derivative in relation to the global curvilinear coordinate applied on each term $\widetilde{\boldsymbol{u}}^{(a)}\left(\boldsymbol{x},\frac{\boldsymbol{\varphi}(\boldsymbol{x})}{\epsilon},p\right)$ from (14), yields the transformation

$$\{\cdot\}_{,j}\equiv\{\cdot\}_{,j}+\frac{\varphi_{l,j}(x)}{\epsilon}\{\cdot\}_{|l} \tag{15}$$

where $\{\cdot\}_{|l}=\frac{\partial}{\partial y_l}\{\cdot\}$ denotes the derivative related to the local curvilinear coordinate.

Replacing (14) into (10), taking into account (15), after some simplifications and grouping in powers of ϵ, the following sequence of problems are obtained

$$\epsilon^{-2}\colon\ \varphi_{l,j}(\boldsymbol{x})(\widetilde{R}^{ijmn}(\boldsymbol{x},\boldsymbol{y},p)\varphi_{s,n}(\boldsymbol{x})\widetilde{u}^{(0)}_{m|s}(\boldsymbol{x},\boldsymbol{y},p))_{|l}=0, \tag{16}$$

$$\begin{aligned}\epsilon^{-1}\colon\ &\varphi_{l,j}(\boldsymbol{x})(\widetilde{R}^{ijmn}(\boldsymbol{x},\boldsymbol{y},p)\varphi_{s,n}(\boldsymbol{x})\widetilde{u}^{(1)}_{m|s}(\boldsymbol{x},\boldsymbol{y},p))_{|l}\\&+(\widetilde{R}^{ijmn}(\boldsymbol{x},\boldsymbol{y},p)\varphi_{s,n}(\boldsymbol{x})\widetilde{u}^{(0)}_{m|s}(\boldsymbol{x},\boldsymbol{y},p))_{,j}\\&+\varphi_{l,j}(\boldsymbol{x})(\widetilde{R}^{ijmn}(\boldsymbol{x},\boldsymbol{y},p)\widetilde{u}^{(0)}_{m,n}(\boldsymbol{x},\boldsymbol{y},p))_{|l}\\&-\varphi_{l,j}(\boldsymbol{x})(\widetilde{R}^{ijmn}(\boldsymbol{x},\boldsymbol{y},p)\Gamma^{r}_{mn}(\boldsymbol{x})\widetilde{u}^{(0)}_{r}(\boldsymbol{x},\boldsymbol{y},p))_{|l}\\&+(\Gamma^{i}_{jk}(\boldsymbol{x})\widetilde{R}^{kjmn}(\boldsymbol{x},\boldsymbol{y},p)+\Gamma^{j}_{jk}(\boldsymbol{x})\widetilde{R}^{ikmn}(\boldsymbol{x},\boldsymbol{y},p))\\&\cdot(\varphi_{s,n}(\boldsymbol{x})\widetilde{u}^{(1)}_{m|s}(\boldsymbol{x},\boldsymbol{y},\boldsymbol{p})+\widetilde{u}^{(0)}_{m,n}(\boldsymbol{x},\boldsymbol{y},p)-\Gamma^{r}_{mn}(\boldsymbol{x})\widetilde{u}^{(0)}_{r}(\boldsymbol{x},\boldsymbol{y},p))\\&+\widetilde{f}^{i}(\boldsymbol{x},p)=0.\end{aligned} \tag{17}$$

$$\begin{aligned}\epsilon^{0}\colon\ &\varphi_{l,j}(\boldsymbol{x})(\widetilde{R}^{ijmn}(\boldsymbol{x},\boldsymbol{y},p)\varphi_{s,n}(\boldsymbol{x})\widetilde{u}^{(2)}_{m|s}(\boldsymbol{x},\boldsymbol{y},p))_{|l}\\&+(\widetilde{R}^{ijmn}(\boldsymbol{x},\boldsymbol{y},p)\varphi_{s,n}(\boldsymbol{x})\widetilde{u}^{(1)}_{m|s}(\boldsymbol{x},\boldsymbol{y},p))_{,j}\\&+\varphi_{l,j}(\boldsymbol{x})(\widetilde{R}^{ijmn}(\boldsymbol{x},\boldsymbol{y},p)\widetilde{u}^{(1)}_{m,n}(\boldsymbol{x},\boldsymbol{y},p))_{|l}\\&+(\widetilde{R}^{ijmn}(\boldsymbol{x},\boldsymbol{y},p)\widetilde{u}^{(0)}_{m,n}(\boldsymbol{x},\boldsymbol{y},p))_{,j}\\&-\varphi_{l,j}(\boldsymbol{x})(\widetilde{R}^{ijmn}(\boldsymbol{x},\boldsymbol{y},p)\Gamma^{r}_{mn}(\boldsymbol{x})\widetilde{u}^{(1)}_{r}(\boldsymbol{x},\boldsymbol{y},p))_{|l}\\&-(\widetilde{R}^{ijmn}(\boldsymbol{x},\boldsymbol{y},p)\Gamma^{r}_{mn}(\boldsymbol{x})\widetilde{u}^{(0)}_{r}(\boldsymbol{x},\boldsymbol{y},p))_{,j}\\&+(\Gamma^{i}_{jk}(\boldsymbol{x})\widetilde{R}^{kjmn}(\boldsymbol{x},\boldsymbol{y},p)+\Gamma^{j}_{jk}(\boldsymbol{x})\widetilde{R}^{ikmn}(\boldsymbol{x},\boldsymbol{y},p))\\&\cdot(\varphi_{s,n}(\boldsymbol{x})\widetilde{u}^{(1)}_{m|s}(\boldsymbol{x},\boldsymbol{y},\boldsymbol{p})+\widetilde{u}^{(0)}_{m,n}(\boldsymbol{x},\boldsymbol{y},p)-\Gamma^{r}_{mn}(\boldsymbol{x})\widetilde{u}^{(0)}_{r}(\boldsymbol{x},\boldsymbol{y},p))\\&+\widetilde{f}^{i}(\boldsymbol{x},p)=0.\end{aligned} \tag{18}$$

Problems (16)–(18) can be solved in recursive form considering the solvability condition reported in Bakhvalov and Panasenko 1989 [10].

Subsequently, a summary for each problem (16)–(18) is proposed.

Problem for ϵ^{-2}

The problem (16) has the trivial solution $\widetilde{\boldsymbol{u}}^{(0)}(\boldsymbol{x},\boldsymbol{y},p)\equiv\mathbf{0}$. Hence, $\widetilde{\boldsymbol{u}}^{(0)}(\boldsymbol{x},\boldsymbol{y},\boldsymbol{p})$ is a solution of (16) if and only if it is constant in relation to the variable $\boldsymbol{y}$ (see Bakhvalov and Panasenko 1989 [10], Persson et al. 1993 [33], Pobedria 1984 [9]). Thus,

$$\widetilde{\boldsymbol{u}}^{(0)}(\boldsymbol{x},\boldsymbol{y},p)=\widetilde{\boldsymbol{v}}(\boldsymbol{x},p), \tag{19}$$

where $\widetilde{\boldsymbol{v}}(\boldsymbol{x},p)$ is a infinitely differentiable function.

Problem for ϵ^{-1}

Considering (19), it is possible to simplify significantly the problem (17). The following terms are vanishing,

$$(\widetilde{R}^{ijmn}(\boldsymbol{x},\boldsymbol{y},p)\varphi_{s,n}(\boldsymbol{x})\widetilde{u}^{(0)}_{m|s}(\boldsymbol{x},\boldsymbol{y},p))_{,j}=0, \tag{20}$$

$$(\Gamma^{i}_{jk}(\boldsymbol{x})\widetilde{R}^{kjmn}(\boldsymbol{x},\boldsymbol{y},p)+\Gamma^{j}_{jk}(\boldsymbol{x})\widetilde{R}^{ikmn}(\boldsymbol{x},\boldsymbol{y},p))(\varphi_{s,n}(\boldsymbol{x})\widetilde{u}^{(0)}_{m|s}(\boldsymbol{x},\boldsymbol{y},p))=0. \tag{21}$$

The problem (17) becomes,

$$\begin{aligned}&\varphi_{l,j}(\boldsymbol{x})(\widetilde{R}^{ijmn}(\boldsymbol{x},\boldsymbol{y},p)\varphi_{s,n}(\boldsymbol{x})\widetilde{u}^{(1)}_{m|s}(\boldsymbol{x},\boldsymbol{y},p))_{|l}\\&=-\varphi_{l,j}(\boldsymbol{x})(\widetilde{R}^{ijmn}(\boldsymbol{x},\boldsymbol{y},p)\widetilde{v}_{m,n}(\boldsymbol{x},p))_{|l}\\&+\varphi_{l,j}(\boldsymbol{x})(\widetilde{R}^{ijmn}(\boldsymbol{x},\boldsymbol{y},p)\Gamma^{r}_{mn}(\boldsymbol{x})\widetilde{v}_{r}(\boldsymbol{x},p))_{|l}.\end{aligned} \tag{22}$$

Using the divergence theorem and the $\mathbf{Y}$-periodicity condition of $\widetilde{R}(\boldsymbol{x},\boldsymbol{y},p)$, the following result can be verified

$$<-\varphi_{l,j}(\boldsymbol{x})(\widetilde{R}^{ijmn}(\boldsymbol{x},\boldsymbol{y},p)\widetilde{v}_{m,n}(\boldsymbol{x},p))_{|l}+\varphi_{l,j}(\boldsymbol{x})(\widetilde{R}^{ijmn}(\boldsymbol{x},\boldsymbol{y},p)\Gamma^{r}_{mn}\widetilde{v}_{r}(\boldsymbol{x},\boldsymbol{p}))_{|l}>=0.$$

The notation $\langle\cdot\rangle$ defines the average over the $\mathbf{Y}$-cell, i.e.,

$$\langle\cdot\rangle:=\frac{1}{\text{meas}(\mathbf{Y})}\int_{\mathbf{Y}}(\cdot)\sqrt{g}\,dy,$$

where meas($\mathbf{Y}$) is the Lebesgue measure of $\mathbf{Y}$, $g=det([g_{ij}])$ and $[g_{ij}]$ is the metric tensor.

The existence and unique solution for the problem (22) is guaranteed. Applying separation of variables to (22), a general solution for (22) can be given

$$\widetilde{u}^{(1)}_{m}(\boldsymbol{x},\boldsymbol{y},p)=\widetilde{N}^{lk}_{m}(\boldsymbol{x},\boldsymbol{y},p)\widetilde{v}_{l}\|_{k}(\boldsymbol{x},p) \tag{23}$$

Developing the covariant derivative and grouping conveniently, (23) can be transformed into

$$\widetilde{u}^{(1)}_{m}(\boldsymbol{x},\boldsymbol{y},p)=\widetilde{N}^{lk}_{(1)m}(\boldsymbol{x},\boldsymbol{y},p)\widetilde{v}_{l,k}(\boldsymbol{x},p)+\widetilde{N}^{p}_{(0)m}(\boldsymbol{x},\boldsymbol{y},p)\widetilde{v}_{p}(\boldsymbol{x},p), \tag{24}$$

where $\widehat{N}^{lk}_{(1)m}\equiv\widehat{N}^{lk}_{m}$ is called *the local function* and $\widehat{N}^{p}_{(0)m}=-\Gamma^{p}_{lk}\widehat{N}^{lk}_{(1)m}$.

Finally, substituting (24) into (22) and after some simplifications the *local problems* in relation to the local functions $\widehat{N}^{lk}_{(1)m}$ and $\widehat{N}^{p}_{(0)m}$ are obtained

$$\varphi_{q,j}(\boldsymbol{x})(\widetilde{R}^{ijmn}(\boldsymbol{x},\boldsymbol{y},p)\varphi_{p,n}(\boldsymbol{x})\widehat{N}^{lk}_{(1)m|p}(\boldsymbol{x},\boldsymbol{y},p)+\widetilde{R}^{ijlk}(\boldsymbol{x},\boldsymbol{y},p))_{|q}=0 \tag{25}$$

$$\varrho_{l,j}(\boldsymbol{x})(\widetilde{R}^{ijmn}(\boldsymbol{x},\boldsymbol{y},p)\varrho_{t,n}(\boldsymbol{x})\widetilde{N}^{p}_{(0)m\,|t}(\boldsymbol{x},\boldsymbol{y},p)-\widetilde{R}^{ijmn}(\boldsymbol{x},\boldsymbol{y},p)\Gamma^{p}_{mn}(\boldsymbol{x}))_{|l}=0 \tag{26}$$

where $\widehat{N}^{lk}_{(1)m}$ is $\mathbf{Y}$-periodic function.

Problem for ϵ^0

The existence of unique $\mathbf{Y}$-periodic solution for the problem (18) is justified if and only if

$$\begin{aligned}
&<(\widetilde{R}^{ijmn}(\boldsymbol{x},\boldsymbol{y},p)\varrho_{s,n}(\boldsymbol{x})\widetilde{u}^{(1)}_{m|s}(\boldsymbol{x},\boldsymbol{y},p))_{j}\\
&+\varrho_{l,j}(\boldsymbol{x})(\widetilde{R}^{ijmn}(\boldsymbol{x},\boldsymbol{y},p)\widetilde{u}^{(1)}_{m,n}(\boldsymbol{x},\boldsymbol{y},p))_{|l}\\
&+(\widetilde{R}^{ijmn}(\boldsymbol{x},\boldsymbol{y},p)\widetilde{u}^{(0)}_{m,n}(\boldsymbol{x},\boldsymbol{y},p))_{j}\\
&-\varrho_{l,j}(\boldsymbol{x})(\widetilde{R}^{ijmn}(\boldsymbol{x},\boldsymbol{y},p)\Gamma^{r}_{mn}(\boldsymbol{x})\widetilde{u}^{(1)}_{r}(\boldsymbol{x},\boldsymbol{y},p))_{|l}\\
&+(\Gamma^{i}_{jk}(\boldsymbol{x})\widetilde{R}^{kjmn}(\boldsymbol{x},\boldsymbol{y},p)+\Gamma^{j}_{jk}(\boldsymbol{x})\widetilde{R}^{ikmn}(\boldsymbol{x},\boldsymbol{y},p))\\
&\cdot(\varrho_{s,n}(\boldsymbol{x})\widetilde{u}^{(1)}_{m|s}(\boldsymbol{x},\boldsymbol{y},p)+\widetilde{u}^{(0)}_{m,n}(\boldsymbol{x},\boldsymbol{y},p)-\Gamma^{r}_{mn}(\boldsymbol{x})\widetilde{u}^{(0)}_{r}(\boldsymbol{x},\boldsymbol{y},p))\\
&-(\widetilde{R}^{ijmn}(\boldsymbol{x},\boldsymbol{y},p)\Gamma^{r}_{mn}(\boldsymbol{x})\widetilde{u}^{(0)}_{r}(\boldsymbol{x},\boldsymbol{y},p))_{,j}+\widetilde{f}^{i}(\boldsymbol{x},p)>=0.
\end{aligned}\tag{27}$$

The functions $\widetilde{\boldsymbol{R}}(\boldsymbol{x},\boldsymbol{y},p)$ and $\widetilde{\boldsymbol{N}}^{lk}(\boldsymbol{x},\boldsymbol{y},p)$ are $\mathbf{Y}$-periodic, hence the divergence theorem leads to the following

$$<\varrho_{l,j}(\boldsymbol{x})(\widetilde{R}^{ijmn}(\boldsymbol{x},\boldsymbol{y},p)\widetilde{u}^{(1)}_{m,n}(\boldsymbol{x},\boldsymbol{y},p))_{|l}>=0,$$

$$<-\varrho_{l,j}(\boldsymbol{x})(\widetilde{R}^{ijmn}(\boldsymbol{x},\boldsymbol{y},p)\Gamma^{r}_{mn}(\boldsymbol{x})\widetilde{u}^{(1)}_{r}(\boldsymbol{x},\boldsymbol{y},\mathrm{p}))_{|l}>=0.$$

Finally, working on (27), the *homogenized problem* is obtained and it can be written in the form

$$\begin{aligned}
&\widetilde{R}^{ijmn}_{(\mathrm{e})}(\boldsymbol{x},p)\widetilde{v}_{m,nj}(\boldsymbol{x},p)+\widetilde{R}^{ilk}_{(\mathrm{e})}(\boldsymbol{x},p)\widetilde{v}_{l,k}(\boldsymbol{x},p)+\widetilde{R}^{il}_{(\mathrm{e})}(\boldsymbol{x},p)\widetilde{v}_{l}(\boldsymbol{x},p)\\
&\quad+\widetilde{f}^{\,i}(\boldsymbol{x},p)=0\quad\text{in}\quad\Omega\times\mathbb{R},
\end{aligned}\tag{28}$$

where the general expressions for the *effective coefficients* are reported,

$$\widetilde{R}^{ijmn}_{(\mathrm{e})}(\boldsymbol{x},p)=<\widetilde{R}^{ijmn}(\boldsymbol{x},\boldsymbol{y},p)+\widetilde{R}^{ijlk}(\boldsymbol{x},\boldsymbol{y},p)\varrho_{p,k}(\boldsymbol{x})\widetilde{N}^{mn}_{(1)l\,|p}(\boldsymbol{x},\boldsymbol{y},p)>,\tag{29}$$

$$\begin{aligned}
\widetilde{R}^{ilk}_{(\mathrm{e})}(\boldsymbol{x},p)=&\widetilde{R}^{ijlk}_{(\mathrm{e}),j}(\boldsymbol{x},p)+\Gamma^{i}_{jh}(\boldsymbol{x})\widetilde{R}^{hjlk}_{(\mathrm{e})}(\boldsymbol{x},p)+\Gamma^{j}_{jh}(\boldsymbol{x})\widetilde{R}^{ihlk}_{(\mathrm{e})}(\boldsymbol{x},p)\\
&-\Gamma^{l}_{mn}(\boldsymbol{x})\widetilde{R}^{ikmn}_{(\mathrm{e})}(\boldsymbol{x},p),
\end{aligned}\tag{30}$$

$$\begin{aligned}
\widetilde{R}^{il}_{(\mathrm{e})}(\boldsymbol{x},p)=&-(\Gamma^{l}_{mn}(\boldsymbol{x})\widetilde{R}^{ijmn}_{(\mathrm{e})}(\boldsymbol{x},p))_{,j}\\
&-(\Gamma^{i}_{jk}(\boldsymbol{x})\widetilde{R}^{kjmn}_{(\mathrm{e})}(\boldsymbol{x},p)+\Gamma^{j}_{jk}(\boldsymbol{x})\widetilde{R}^{ikmn}_{(\mathrm{e})}(\boldsymbol{x},p))\Gamma^{l}_{mn}(\boldsymbol{x}).
\end{aligned}\tag{31}$$

The boundary conditions for the homogenized problem (28)–(31) are rewritten replacing (14) into (11) and (12), respectively. Applying the average operator, we obtain

$$\widetilde{v}_{i}(\boldsymbol{x},p)=u_{i}{}^{0}\,\text{on}\,\Sigma_{1}\times[0,+\infty),\tag{32}$$

$$\begin{aligned}
&(\widetilde{R}^{ijkl}_{(\mathrm{e})}(\boldsymbol{x},p)v_{k,l}(\boldsymbol{x},p)-\Gamma^{k}_{mn}(\boldsymbol{x})\widetilde{R}^{ijmn}_{(\mathrm{e})}(\boldsymbol{x},p)v_{k}(\boldsymbol{x},p))n_{j}\\
&\quad=s^{i}_{0}\,\text{on}\,\Sigma_{2}\times[0,+\infty).
\end{aligned}\tag{33}$$

The initial condition is taken from (13)

$$\widetilde{v}_{i}(\boldsymbol{x},0)=0,\quad\text{in}\quad\Omega\times\{0\}.\tag{34}$$

The expressions (16)–(18), the local problems (25) and (26), the homogenized problem (28) and the effective coefficients (29)–(31) coincide with the reported in Cruz-González et al. 2018 [34] when $\boldsymbol{\varrho}(x)$ is the identity function (i.e. $\varrho_{l,j}=\delta_{lj}$) and we are in the presence of a Cartesian coordinate system.

4. Effective viscoelastic coefficients for stratified composites

The stratified composites are those for which a property of the material is periodic in relation to $\boldsymbol{y}=\frac{\boldsymbol{\varrho}(\boldsymbol{x})}{\epsilon}$ and the parametric equation $\varrho(\boldsymbol{x})$= constant describes the surfaces into the structure. The present study is focused on the relaxation modulus property. Besides, the stratified function satisfies $\boldsymbol{\varrho}$: $\mathbb{R}^n\to\mathbb{R}^m$ with $n>m$ (see Tsalis et al. 2012 [26]). The layered structures are an example of stratified composites when stratified function are defined as ϱ: $\mathbb{R}^n\to\mathbb{R}^1$ with $n=2,3$. Many effects can be obtained with the use of stratified functions, waviness and variation of thickness are examples of them.

4.1. Curvilinear laminated composite

Now, the stratified function $\varrho(x_1,x_2,x_3)=x_3$ is assumed. The axis x_3 describes the periodicity of the layers and $y=\frac{x_3}{\epsilon}$ is verified. Therefore, the relaxation modulus $R(\boldsymbol{x},y,t)$ is regular in the variables x and periodic in y. The local problem (25) is transformed as follows,

$$\frac{\partial}{\partial y}\left(\widetilde{R}^{i3k3}(\boldsymbol{x},y,p)\frac{\partial\widetilde{N}^{rs}_{(1)k}(\boldsymbol{x},y,p)}{\partial y}+\widetilde{R}^{i3rs}(\boldsymbol{x},y,p)\right)=0,\tag{35}$$

$$\widetilde{R}^{i3k3}(\boldsymbol{x},y,p)\frac{\partial\widetilde{N}^{rs}_{(1)k}(\boldsymbol{x},y,p)}{\partial y}+\widetilde{R}^{i3rs}(\boldsymbol{x},y,p)=\widetilde{A}^{i3rs}(\boldsymbol{x},p).\tag{36}$$

The average operator is applied on both sides of (36) and taking into account the periodicity condition of $\widehat{N}^{rs}_{(1)k}$, the following expression is obtained

$$\widetilde{A}^{i3rs}(\boldsymbol{x},p)=<(\widetilde{R}^{i3q3}(\boldsymbol{x},y,p))^{-1}>^{-1}<(\widetilde{R}^{p3q3}(\boldsymbol{x},y,p))^{-1}\widetilde{R}^{p3rs}(\boldsymbol{x},y,p)>.\tag{37}$$

Substituting (37) into (36) and after some simplifications

$$\begin{aligned}
\tfrac{\partial\widetilde{N}^{rs}_{(1)k}(\boldsymbol{x},y,p)}{\partial y}=&(\widetilde{R}^{l3k3}(\boldsymbol{x},y,p))^{-1}<(\widetilde{R}^{l3q3}(\boldsymbol{x},y,p))^{-1}>^{-1}\\
\cdot&<(\widetilde{R}^{p3q3}(\boldsymbol{x},y,p))^{-1}\widetilde{R}^{p3rs}(\boldsymbol{x},y,p)>-(\widetilde{R}^{l3k3}(\boldsymbol{x},y,p))^{-1}\widetilde{R}^{l3rs}(\boldsymbol{x},y,p).
\end{aligned}\tag{38}$$

Replacing (38) into (29), the general expression of the effective coefficients for curvilinear laminated composites in Laplace-Carson space is given

$$\begin{aligned}
\widetilde{R}^{ijrs}_{(\mathrm{e})}(\boldsymbol{x},p)=&<\widetilde{R}^{ijrs}(\boldsymbol{x},y,p)>+<\widetilde{R}^{ijk3}(\boldsymbol{x},y,p)(\widetilde{R}^{l3k3}(\boldsymbol{x},y,p))^{-1}>\\
\cdot&<(\widetilde{R}^{l3q3}(\boldsymbol{x},y,p))^{-1}>^{-1}<(\widetilde{R}^{p3q3}(\boldsymbol{x},y,p))^{-1}\widetilde{R}^{p3rs}(\boldsymbol{x},y,p)>\\
-&<\widetilde{R}^{ijk3}(\boldsymbol{x},y,p)(\widetilde{R}^{l3k3}(\boldsymbol{x},y,p))^{-1}\widetilde{R}^{l3rs}(\boldsymbol{x},y,p)>.
\end{aligned}\tag{39}$$

The relaxation modulus in time space, when the viscoelastic response of the microstructure constituents is assumed to be isotropic, can be expressed in the form

$$R^{ijkl}(\boldsymbol{x},y,t)=\lambda(\boldsymbol{x},t)g^{ij}(y)g^{kl}(y)+\mu(\boldsymbol{x},t)(g^{ik}(y)g^{jl}(y)+g^{il}(y)g^{jk}(y)),\tag{40}$$

where $\lambda(\boldsymbol{x},t)$ and $\mu(\boldsymbol{x},t)$ are the relaxation functions and $[g^{ij}]=[g_{ij}]^{-1}$.

Consequently, if the coordinate system x is orthogonal, substituting (40) into (39), the analytical expressions for the effective coefficients are obtained

$$\begin{aligned}
\widetilde{R}^{1111}_{(\mathrm{e})}(\boldsymbol{x},p)=&<\widetilde{R}^{1111}(\boldsymbol{x},y,p)>-\left\langle\frac{(\widetilde{R}^{1133}(\boldsymbol{x},y,p))^{2}}{\widetilde{R}^{3333}(\boldsymbol{x},y,p)}\right\rangle\\
&+\left\langle\frac{\widetilde{R}^{1133}(\boldsymbol{x},y,p)}{\widetilde{R}^{3333}(\boldsymbol{x},y,p)}\right\rangle^{2}<(\widetilde{R}^{3333}(\boldsymbol{x},y,p))^{-1}>^{-1}
\end{aligned}\tag{41}$$

$$\begin{aligned}
\widetilde{R}^{1122}_{(\mathrm{e})}(\boldsymbol{x},p)=&<\widetilde{R}^{1122}(\boldsymbol{x},y,p)>\\
&+\left\langle\frac{\widetilde{R}^{1133}(\boldsymbol{x},y,p)}{\widetilde{R}^{3333}(\boldsymbol{x},y,p)}\right\rangle<(\widetilde{R}^{3333}(\boldsymbol{x},y,p))^{-1}>^{-1}\cdot\\
&\left\langle\frac{\widetilde{R}^{2233}(\boldsymbol{x},y,p)}{\widetilde{R}^{3333}(\boldsymbol{x},y,p)}\right\rangle-\left\langle\frac{\widetilde{R}^{1133}(\boldsymbol{x},y,p)\widetilde{R}^{2233}(\boldsymbol{x},y,p)}{\widetilde{R}^{3333}(\boldsymbol{x},y,p)}\right\rangle,
\end{aligned}\tag{42}$$

$$\widetilde{R}^{1133}_{(\mathrm{e})}(\boldsymbol{x},p)=<\widetilde{R}^{1133}(\boldsymbol{x},y,p)(\widetilde{R}^{3333}(\boldsymbol{x},y,p))^{-1}><(\widetilde{R}^{3333}(\boldsymbol{x},y,p))^{-1}>^{-1},\tag{43}$$

$$\widetilde{R}^{2233}_{(e)}(\boldsymbol{x},p) = <\widetilde{R}^{2233}(\boldsymbol{x},y,p)(\widetilde{R}^{3333}(\boldsymbol{x},y,p))^{-1}><(\widetilde{R}^{3333}(\boldsymbol{x},y,p))^{-1}>^{-1}, \tag{44}$$

$$\widetilde{R}^{2222}_{(e)}(\boldsymbol{x},p) = <\widetilde{R}^{2222}(\boldsymbol{x},y,p)> - \left\langle \frac{(\widetilde{R}^{2233}(\boldsymbol{x},y,p))^2}{\widetilde{R}^{3333}(\boldsymbol{x},y,p)} \right\rangle + \left\langle \frac{\widetilde{R}^{2233}(\boldsymbol{x},y,p)}{\widetilde{R}^{3333}(\boldsymbol{x},y,p)} \right\rangle^2 <(\widetilde{R}^{3333}(\boldsymbol{x},y,p))^{-1}>^{-1} \tag{45}$$

$$\widetilde{R}^{3333}_{(e)}(\boldsymbol{x},p) = <(\widetilde{R}^{3333}(\boldsymbol{x},y,p))^{-1}>^{-1}, \tag{46}$$

$$\widetilde{R}^{2323}_{(e)}(\boldsymbol{x},p) = <(\widetilde{R}^{2323}(\boldsymbol{x},y,p))^{-1}>^{-1}, \tag{47}$$

$$\widetilde{R}^{1313}_{(e)}(\boldsymbol{x},p) = <(\widetilde{R}^{1313}(\boldsymbol{x},y,p))^{-1}>^{-1}, \tag{48}$$

$$\widetilde{R}^{1212}_{(e)}(\boldsymbol{x},p) = <(\widetilde{R}^{1212}(\boldsymbol{x},y,p))>. \tag{49}$$

The expressions (41)–(49) when the metric tensor is $[g_{ij}] = [\delta_{ij}]$ (Cartesian coordinates system), coincide with the reported in Cruz-González et al. 2018 [34].

4.2. A general form of stratified functions

The main objective of this section is to provide a methodology in order to find formulas for the effective coefficients when the stratified function is being $\varrho\colon \mathbb{R}^2 \to \mathbb{R}$. Considering an orthogonal curvilinear coordinate system x, each constituent with isotropic behavior, $\varrho \equiv \varrho(\boldsymbol{x})$ and using the Voigt notation, the expression of the effective coefficients (29) becomes

$$\begin{aligned}\widetilde{R}^{ijmn}_{(e)}(\boldsymbol{x},p) \equiv \widetilde{R}^{\alpha\beta}_{(e)}(\boldsymbol{x},p) = <&\widetilde{R}^{\alpha\beta}(\boldsymbol{x},y,p) + (\widetilde{R}^{\alpha1}(\boldsymbol{x},y,p)\varrho_{,1}(\boldsymbol{x}) \\ &+ \widetilde{R}^{\alpha6}(\boldsymbol{x},y,p)\varrho_{,2}(\boldsymbol{x}) + \widetilde{R}^{\alpha5}(\boldsymbol{x},y,p)\varrho_{,3}(\boldsymbol{x}))\frac{\partial\widetilde{N}^{\beta}_{(1)1}(\boldsymbol{x},y,p)}{\partial y} + (\widetilde{R}^{\alpha6}(\boldsymbol{x},y,p)\varrho_{,1}(\boldsymbol{x}) \\ &+ \widetilde{R}^{\alpha2}(\boldsymbol{x},y,p)\varrho_{,2}(\boldsymbol{x}) + \widetilde{R}^{\alpha4}(\boldsymbol{x},y,p)\varrho_{,3}(\boldsymbol{x}))\frac{\partial\widetilde{N}^{\beta}_{(1)2}(\boldsymbol{x},y,p)}{\partial y} + (\widetilde{R}^{\alpha5}(\boldsymbol{x},y,p)\varrho_{,1}(\boldsymbol{x}) \\ &+ \widetilde{R}^{\alpha4}(\boldsymbol{x},y,p)\varrho_{,2}(\boldsymbol{x}) + \widetilde{R}^{\alpha3}(\boldsymbol{x},y,p)\varrho_{,3}(\boldsymbol{x}))\frac{\partial\widetilde{N}^{\beta}_{(1)3}(\boldsymbol{x},y,p)}{\partial y} \Big\rangle.\end{aligned} \tag{50}$$

The local problem (25) is transformed into the following differential equations system ($\beta = 1,\ 2,\ ...,\ 6$)

$$\begin{aligned}\frac{\partial}{\partial y}\Big(&\varrho_{,1}(\boldsymbol{x})\widetilde{R}^{1\beta}(\boldsymbol{x},y,p) + \varrho_{,2}(\boldsymbol{x})\widetilde{R}^{6\beta}(\boldsymbol{x},y,p) + (\varrho_{,1}(\boldsymbol{x})\widetilde{R}^{11}(\boldsymbol{x},y,p)\varrho_{,1}(\boldsymbol{x}) \\ &+ \varrho_{,2}(\boldsymbol{x})\widetilde{R}^{66}(\boldsymbol{x},y,p)\varrho_{,2}(\boldsymbol{x}))\frac{\partial\widetilde{N}^{\beta}_{(1)1}(\boldsymbol{x},y,p)}{\partial y} + (\varrho_{,1}(\boldsymbol{x})\widetilde{R}^{12}(\boldsymbol{x},y,p)\varrho_{,2}(\boldsymbol{x}) \\ &+ \varrho_{,2}(\boldsymbol{x})\widetilde{R}^{66}(\boldsymbol{x},y,p)\varrho_{,1}(\boldsymbol{x}))\frac{\partial\widetilde{N}^{\beta}_{(1)2}(\boldsymbol{x},y,p)}{\partial y}\Big) = 0,\end{aligned} \tag{51}$$

$$\begin{aligned}\frac{\partial}{\partial y}\Big(&\varrho_{,1}(\boldsymbol{x})\widetilde{R}^{6\beta}(\boldsymbol{x},y,p) + \varrho_{,2}(\boldsymbol{x})\widetilde{R}^{2\beta}(\boldsymbol{x},y,p) + (\varrho_{,1}(\boldsymbol{x})\widetilde{R}^{66}(\boldsymbol{x},y,p)\varrho_{,2}(\boldsymbol{x}) \\ &+ \varrho_{,2}(\boldsymbol{x})\widetilde{R}^{21}(\boldsymbol{x},y,p)\varrho_{,1}(\boldsymbol{x}))\frac{\partial\widetilde{N}^{\beta}_{(1)1}(\boldsymbol{x},y,p)}{\partial y} + (\varrho_{,1}(\boldsymbol{x})\widetilde{R}^{66}(\boldsymbol{x},y,p)\varrho_{,1}(x) \\ &+ \varrho_{,2}(\boldsymbol{x})\widetilde{R}^{22}(\boldsymbol{x},y,p)\varrho_{,2}(\boldsymbol{x}))\frac{\partial\widetilde{N}^{\beta}_{(1)2}(\boldsymbol{x},y,p)}{\partial y}\Big) = 0,\end{aligned} \tag{52}$$

$$\begin{aligned}\frac{\partial}{\partial y}\Big(&\varrho_{,1}(\boldsymbol{x})\widetilde{R}^{5\beta}(\boldsymbol{x},y,p) + \varrho_{,2}(x)\widetilde{R}^{4\beta}(\boldsymbol{x},y,p) + (\varrho_{,1}(\boldsymbol{x})\widetilde{R}^{55}(\boldsymbol{x},y,p)\varrho_{,1}(\boldsymbol{x}) \\ &+ \varrho_{,2}(\boldsymbol{x})\widetilde{R}^{44}(\boldsymbol{x},y,p)\varrho_{,2}(\boldsymbol{x}))\frac{\partial\widetilde{N}^{\beta}_{(1)3}(\boldsymbol{x},y,p)}{\partial y}\Big) = 0.\end{aligned} \tag{53}$$

The system (51)–(53) can be solved integrating each equation in relation to the local variable and determining the constants of integration. The expressions $\frac{\partial\widetilde{N}^{\beta}_{(1)i}}{\partial y}$ with $i = 1, 2, 3$, once calculated, they can be substituted into (50) to find the effective coefficients.

4.3. Relation between effective relaxation modulus and effective creep compliance

The mathematical relationship between effective relaxation modulus and effective creep compliance, given in the Laplace-Carson space, is proposed in Hashin 1972 [35] as follows

$$\widehat{R}^{ijmn}_{(e)}(p)\widehat{J}^{mnkl}_{(e)}(p) = I^{ijkl}, \tag{54}$$

where I^{ijkl} is the 4to order identity tensor.

Applying the inverse of Laplace-Carson transform on (54) and considering the convolution theorem, it leads to the convolution Stieltjes integral (see Hanyga and Seredyńska 2007 [36])

$$\int_0^t \boldsymbol{R}_{(e)}(\tau)J_{(e)}(t-\tau)d\tau = t\boldsymbol{I}, \qquad t > 0. \tag{55}$$

Therefore, if the effective relaxation modulus is known, there is a way to calculate the effective creep compliance in Laplace-Carson space using (54). Finally, applying the inversion of Laplace-Carson transform, it returns to the temporal space. This process includes to solve a system of 81 equations, as many times as points in time space we are considering.

The MATLAB's functions INVLAP and GAVSTEH developed by Hollenbeck 1998 [37] and Srigutomo 2006 [38], respectively are used in the inversion of Laplace-Carson transform. The algorithms can transform functions of complex variable s^{α}, where α is a real exponent. They can also transform functions which contain rational, irrational and transcendent expressions. As a negative aspect, they present problems close to zero.

5. Applications to multilayered composite materials

The results of previous sections allow to calculate the effective viscoelastic properties of composite materials with different geometrical shapes using the stratified functions and curvilinear coordinates. Even if we use these two properties separately, it's possible to analyze from both points of view the effective behavior of a same structure. The composite material shown in Fig. 1 b) can be modeled considering the following schemes.

(A) Cartesian coordinates $\boldsymbol{x} = (x_1, x_2, x_3)$ and stratified function $\varrho_1(x_1, x_2) = \sqrt{x_2^2 + x_1^2}$.
(B) Cylindrical coordinate $\boldsymbol{x} = (\theta, r, z)$ and stratified function $\varrho_2(\theta, r) = r$.

The first one involves the resolution of the local problem (51)–(53) and afterwards the effective coefficient (50). The second one operates with expressions (41)–(49). In this case, is less complex to perform the calculations using the scheme (B). The operator that appears between the formulas (22) and (23), suitable to the cylindrical coordinates, is used for that purpose.

$$\langle F \rangle = \frac{2}{R_2^2 - R_0^2}\int_{R_0}^{R_2} F{\cdot}rdr. \tag{56}$$

Also, in certain cases, the stratified functions are better to use instead of curvilinear coordinates. For example, elliptical shapes can be describing through Cartesian coordinates $\boldsymbol{x} = (x_1, x_2, x_3)$ and stratified function $\varrho\left(x_1, x_2\right) = \sqrt{\left(\frac{x_2}{a}\right)^2 + \left(\frac{x_1}{b}\right)^2}$. Nevertheless, it is not possible to use with other common coordinate systems.

Therefore, interacting with these two schemes, we can get a more general design as shown in Fig. 1 a).

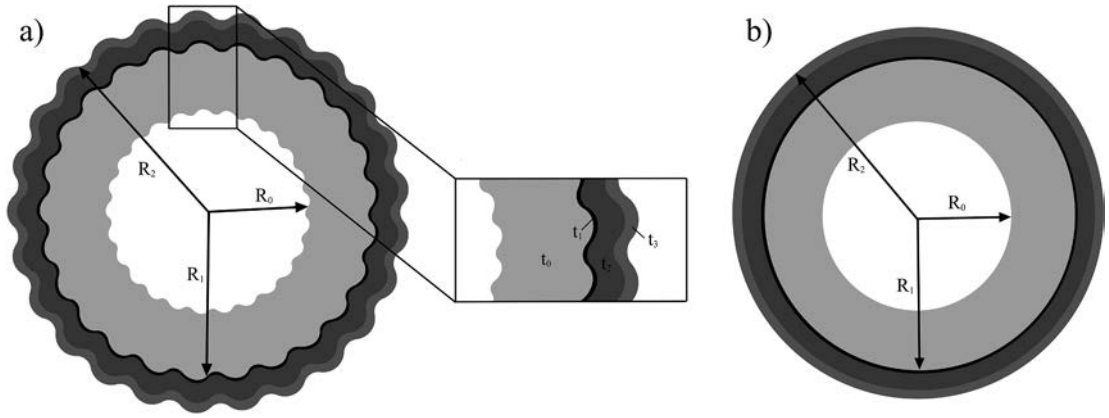

Fig. 1. Examples of concentric laminated viscoelastic models. a) Wavy and b) not wavy laminated composite in cylindrical coordinates. t_0, t_1, t_2 and t_3 represent the thickness for each layer.

5.1. Wavy laminated composites in cylindrical coordinates

A recent activity in cylindrical geometry structures is motivated for engineering, structural and biomechanical applications (see Araújo-Cavalcante et al. 2011 [39], Guinovart-Sanjuán et al. 2016 [29]). For example, the composite materials with carbon nanotubes, the study of bones, the modeling of the aorta, among others. On the other hand, wavy effects haven't been studied enough (see Araújo-Cavalcante & Cavalcanti-Marques 2017 [40]) but they are present in a variety of natural biological systems (Liao and Vesely 2003 [41]) and in civil engineering applications (see Katz et al. 2015 [42]) to name a few.

At this point, the calculation of the effective viscoelastic properties for a laminated composite material with cylindrical geometry, wavy effects and isotropic response is developed (see Fig. 1 a)). This particular case can be modeled with the scheme,

(C) cylindrical coordinate $\boldsymbol{x} = (\theta, r, z)$ and stratified function $\varsigma_3\left(\theta, r\right) = r - \frac{H}{n}\sin\left(\frac{2\pi n\theta}{L}\right)$,

where H is the parameter related to the oscillation, L is the length of the unit cell (see Tsalis et al. 2012 [26]), the amplitude-to-wavelength ratio is $\frac{H}{L} = \frac{1}{2\pi}$ and the term n represents the number of waviness for $0 \leqslant \theta \leq 2\pi$. It is really worthy to note, when n is fixed and r is sufficiently biggest, waviness of Fig. 1 a) dissipate and hence, it looks like the shape of Fig. 1 b).

Then, assuming that the relaxation functions in each layer satisfy the following three parameters model (see Liu et al. 2004 [43])

$$\mu_i(t) = q_{0i} + q_{1i}e^{-p_i t},$$

$$\lambda_i(t) = K_i - \frac{2}{3}\mu_i(t), \quad i = 0, \ldots, 3.$$

The respective values for the constants of the model are shown in Table 1. In addition, are known $R_0 = 0.62$ cm, $R_1 = 1.02$ cm, $R_2 = 1.22$ cm and the thicknesses $t_0 = 0.4$ cm, $t_1 = 0.02$ cm, $t_2 = 0.12$ cm, $t_3 = 0.06$ cm.

The metric tensor associated to (A) satisfies $[g_{ij}] = [\delta_{ij}]$. In relation to (B) and (C), the metric tensor and its inverse becomes

$$[g_{ij}] = \begin{bmatrix} r^2 & 0 & 0 \\ 0 & 1 & 0 \\ 0 & 0 & 1 \end{bmatrix}, \qquad [g^{ij}] = \begin{bmatrix} \frac{1}{r^2} & 0 & 0 \\ 0 & 1 & 0 \\ 0 & 0 & 1 \end{bmatrix}$$

where $det\,[g_{ij}] = r^2$. Moreover, the non-zero Christoffel symbols are calculated,

$$\Gamma^3_{11} = -r, \quad \Gamma^1_{13} = \Gamma^1_{31} = \frac{1}{r}.$$

The geometrical shape of the Fig. 1 a) yields the next transformation in the average operator

$$C_1 = \int_0^{2\pi}\left(\int_{R_0-\frac{H}{n}\sin\left(\frac{2\pi n\theta}{L}\right)}^{R_2-\frac{H}{n}\sin\left(\frac{2\pi n\theta}{L}\right)} rdr\right)d\theta, \qquad \langle F\rangle = \frac{1}{C_1}\int_0^{2\pi}\left(\int_{R_0-\frac{H}{n}\sin\left(\frac{2\pi n\theta}{L}\right)}^{R_2-\frac{H}{n}\sin\left(\frac{2\pi n\theta}{L}\right)} F\cdot rdr\right)d\theta. \tag{57}$$

The calculation of the effective viscoelastic properties is performed using the different approaches analyzed above. The AHM with the scheme (C) for $n = 25$ is applied on Fig. 1 a). The formulas (50), (51)–(53) and (57) are used in the process. Also, AHM and FEM both with the scheme (B) are proposed for Fig. 1 b). In this case, the AHM is carried out using the Eqs. (41)–(49). On the other hand, the finite element method is used to solve problems (35) in order to compute the effective coefficients using (29). For that purpose, since these problems are one dimensional and défend on the interval [R1,R2] for x and p fixed, piecewise linear shape functions are considered to solve the problems on the whole interval (Equivalent Single Layer formulation). One hundred nodes are used on [R1,R2] to discretize the problem, because we have observed that this number of nodes are sufficient to obtain a convergence on the effective coefficients. The expression (38), the transformations in the Eq. (40) induced by the cylindrical coordinates and the use of the average operator (56) are considered. Some comparisons are displayed in Fig. 2 and they exhibit a good agreement between the two approaches. Both methods are set as tools for calculating the effective viscoelastic properties. The AHM with the analytical set of explicit formulas allows calculation with very low computational cost and effort in a very short time. However, for more general stratified functions in the form $\boldsymbol{\varsigma}$: $\mathbb{R}^3 \to \mathbb{R}^3$, the local problems are not solvable analytically and the method fails. Then, the numerical approach in connection with FEM let to solve this challenging. Also, the figures show the influence that the design of the structure and the different effects, such as waviness, have on the results.

Table 1
Material constants for the three parameters model.

Layers	K (GPa)	q_0 (GPa)	q_1 (GPa)	p (1/day)
Layer 0	259.65e8	1.785e8	0.69e8	0.002665
Layer 1	628.2e8	9.67e8	3.22e8	0.00658
Layer 2	108.9e8	6.1e8	1.84e8	0.00125
Layer 3	368.55e8	7.885e8	2.53e8	0.003915

5.2. Double homogenization. Wavy composite material reinforced with long rectangular fibers

Fiber reinforced composites are widely used in high performance

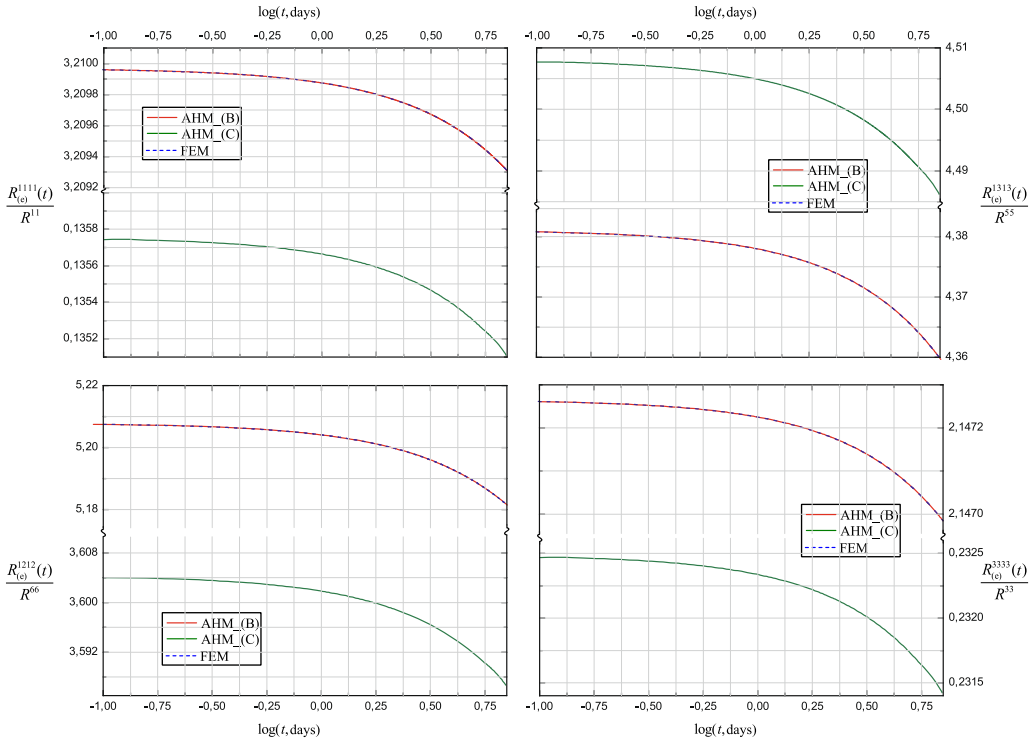

Fig. 2. Computation of the effective relaxation modulus. Comparison between MHA and FEM. The numerical values have been normalized, (a) $R^{11} = 10^{10}$, (b) $R^{55} = 10^{8}$, (c) $R^{66} = 10^{10}$ and (d) $R^{33} = 10^{10}$.

structural applications due to their better mechanical properties and high strength to weight ratio (see Saravanakumar et al. 2018 [44]). As example, the glass-fiber reinforced composites find applications in the industry of wind turbine's blades and impeller elements (see Martynenko and Lvov 2017 [45]). Besides, composites fabricated with brittle epoxy matrix inherently has low fracture toughness and weak fiber/matrix interface bond strength (see Saravanakumar et al. 2018 [44]). On the other hand, their use requires a highly accurate knowledge of material properties because of the apparition of internal stresses and several imperfections like fiber waviness. These phenomena constitute an important aspect in the manufacturing of thick composites with long fibers (see Jochum et al. 2008 [46]).

In this section, a composite material reinforced with long rectangular fibers, distributed periodically along axis x_3 and both, the structure and the fibers, with wavy effect is considered (see Fig. 3). According to geometrical configuration of the structure, the two-steps homogenization scheme in different directions can be used to estimate the overall effective behavior (see Otero et al. 2003 [47] and Guinovart-Sanjuán et al. 2018 [48]). In this example, elastic fibers (glass) are embedded in a viscoelastic matrix (epoxy). The viscoelastic material can be modelled using normalized Prony series, based on the generalized Maxwell's model

$$\mu(t) = \mu_0\left(1 - \sum_{n=1}^{N} g_n\left(1 - e^{(-t/\tau_n)}\right)\right), \tag{58}$$

$$K(t) = K_0\left(1 - \sum_{m=1}^{M} k_m\left(1 - e^{(-t/\tau_m)}\right)\right), \tag{59}$$

where $\mu(t)$ and $k(t)$ are time dependent relaxation shear and relaxation bulk modulus; μ_0 and K_0 are instantaneous shear and bulk modulus; g_n, k_m and τ_i are parameters fitted through experimental tests (see Zhang and Ostoja-Starzewski 2015 [49] and 2016 [50]). Mechanical properties of materials can be found in Tables 2 and 3, respectively. For sake of simplicity in the model, only one term in the Prony series (see Pathan et al. 2017 [51]) is considered.

The stratification function which describes the microstructure and the wavy effect, is given as follows (see Guinovart-Sanjuán et al. 2016 [29])

$$\varphi\left(x_1, x_2\right) = x_2 - H\sin\left(\frac{2\pi x_1}{L}\right). \tag{60}$$

The average operator is calculated

$$\langle f \rangle = V_1 f_{(1)} + V_2 f_{(2)}, \tag{61}$$

where the subscripts (1), (2) are indicating the corresponding material andV_i represents the volume fractions of each constituent.

The two-steps homogenization scheme is dealt below:

1. Conveniently, the composite material is homogenized in the direction of axis x_3. The structure is analyzed as a two-layered medium with transversely isotropic properties (see Fig. 3 (a)). The calculation of the effective viscoelastic coefficients is performed using the Eqs. (41)–(49). Moreover, the subscript (e_1) is added indicating the first homogenization (see Fig. 3 (a)).
2. The resulting structure is displayed in Fig. 3 (b)). It represents a new two-layered medium with wavy effects. The effective coefficients are calculated using the stratified function (60) and the formulas (50) and (51)–(53). The subscript (e_2) is proposed to denote the second homogenization (Fig. 3 (b)). Besides, the average operator (61) is transformed into $\langle f \rangle = V_1 f_{(e_1)} + V_2 f_{(2)}$; where the subscript(2) represents the property of the viscoelastic matrix and the subscript (e_1) denotes the effective viscoelastic property obtained in the first homogenization step (Fig. 3 (b)).

The mathematical problems for modeling rectangular-cross-section fibrous composites can not be solved using analytical methods. The double homogenization method here described is an alternative to offer easy-handle analytical formulas for simulate the macroscopic behavior of such composites. Fig. 3 (a) and (b) illustrate the general procedure carried out in this work. Furthermore, the method can not be applied

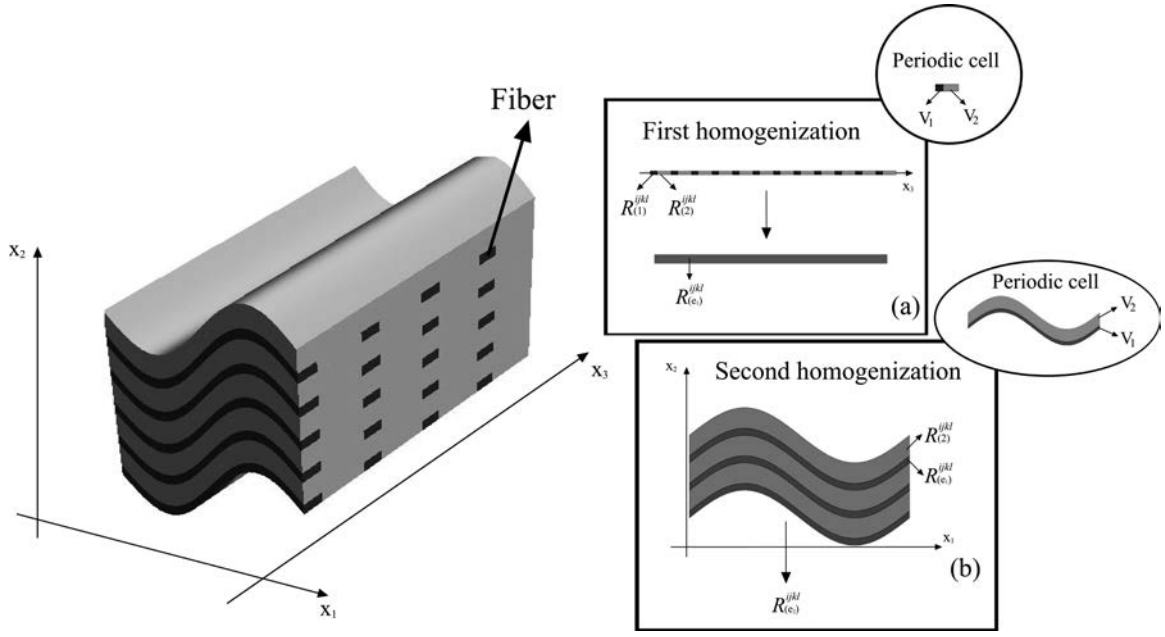

Fig. 3. Periodic cell for the laminated structure with wavy effect.

Table 2
Mechanical properties for the constituents of the composite material.

	Young modulus (GPa)	Poisson ratio
Epoxy	2.76	0.38
Glass fibre	50	0.2

Table 3
Coefficients of the Prony series.

	g_1	k_1	τ_1 (s)
Epoxy	0.6	0.6	20

when the fibers are circular or elliptical.

The outcomes in the calculation of the effective relaxation modulus and the effective creep compliance are displayed in Fig. 4. The methodology allows to estimate the effective behavior for a composite material with long rectangular fibers and wavy effects. The process to obtain the effective relaxation modulus was explained previously in the two-steps homogenization scheme. On the other hand, the effective creep compliance is found using the Eq. (54) and the performance of the numerical inversion of Laplace-Carson transform.

6. Conclusions

In this article, previous results on the field of elastic materials are extended to non-ageing viscoelastic ones by using the correspondence principle and the Laplace-Carson transform. More general expressions for the local problems, the homogenized problem and the effective coefficients in non-ageing linear viscoelastic composite materials with generalized periodicity are obtained. The stratified functions and the curvilinear coordinate system are included in the analysis allowing to study new features in the structures. The multi-step homogenization scheme is performed to estimate the overall behavior for a viscoelastic composite material reinforced with long rectangular fibers and wavy effects. A numerical algorithm for computing the effective creep compliance has been developed and the numerical implementation for the calculations of the effective relaxation modulus has been established. The comparisons with FEM display good agreements between the two approaches. Also, the AHM shows to be a good alternative for obtaining results with low computational cost and good accuracy by using the

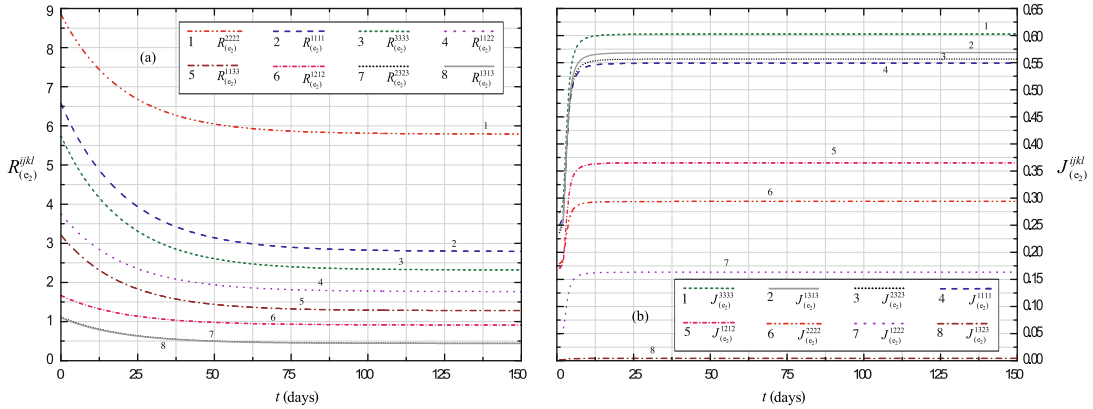

Fig. 4. (a) Computation of the effective relaxation modulus for a composite material with long rectangular fibers and wavy effects, using double homogenization. (b) Taking into account (54), the effective creep compliance is obtained. Volume fractions $V_1 = 0.3$, $V_2 = 0.7$, amplitude-to-wavelength ratio of 0.5 and the value $x_1 = 1$ are considered.

analytical set of formula. This approach offers an effective technique for investigating both macroscopic and microscopic properties of periodic structures. The main disadvantage is set when the local problems are not solvable analytically and the numerical solution of cell problems is required.

Acknowledgements

The partial results of this work were presented in the plenary lectures of the 4th International Conference on Mechanics of Composites held 9–12 July 2018 at the University Carlos III Madrid, Spain. RR would like to thank MyM-IIMAS-UNAM and PREI-DGAPA-UNAM for financial support. Also, FJS thanks funding from DGAPA, UNAM. This work was supported by the project PAPIIT-DGAPA-UNAM IA100919. The authors are thankful to Ana Pérez Arteaga and Ramiro Chávez Tovar for technical assistance. OLCG kindly thanks to Ecole Doctorale no. 353 de L'Université de Aix Marseille and L'équipe Matériaux & Structures du Laboratoire de Mécanique et d'Acoustique LMA - UMR 7031 AMU - CNRS - Centrale Marseille 4 impasse Nikola Tesla CS 40006 13453 Marseille Cedex 13, France.

References

[1] Maghous S, Creus GJ. Periodic homogenization in thermoviscoelasticity: case of multilayered media with ageing. Int J Solids Struct 2003;40(4):851–70. https://doi.org/10.1016/S0020-7683(02)00549-8.
[2] Kalamkarov AL, Andrianov IV, Danishevs'kyy VV. Asymptotic homogenization of composite materials and structures. Appl Mech Rev 2009;62(3):1–20. https://doi.org/10.1115/1.3090830.
[3] Sevostianov I, Giraud A. Generalization of maxwell homogenization scheme for elastic material containing inhomogeneities of diverse shape. Int J Eng Sci 2013;64:23–36. https://doi.org/10.1016/j.ijengsci.2012.12.004.
[4] Sevostianov I, Levin V, Radi E. Effective properties of linear viscoelastic microcracked materials: Application of maxwell homogenization scheme. Mech Mater 2015;84:28–43. https://doi.org/10.1016/j.mechmat.2015.01.004.
[5] Honorio T, Bary B, Sanahuja J, Benboudjema F. Effective properties of n-coated composite spheres assemblage in an ageing linear viscoelastic framework. Int J Solids Struct 2017;124:1–13. https://doi.org/10.1016/j.ijsolstr.2017.04.028.
[6] Schöneich M, Dinzart F, Sabar H, Berbenni S, Stommel M. A coated inclusion-based homogenization scheme for viscoelastic composites with interphases. Mech Mater 2017;105:89–98. https://doi.org/10.1016/j.mechmat.2016.11.009.
[7] Bensoussan A, Papanicolau G, Lions J-L. Asymptotic Analysis for Periodic Structures, 1st ed., vol. 5, North-Holland; 1978.
[8] Sanchez-Palencia E. Non-homogeneous media and vibration theory, lecture notes in physics. Springer-Verlag; 1980.
[9] Pobedria B. Mechanics of composite materials. Moscow State University Press; 1984.
[10] Bakhvalov NS, Panasenko G. Homogenisation: averaging processes in periodic media: mathematical problems in the mechanics of composite materials, mathematics and its applications. Kluwer Academic Publishers; 1989.
[11] Oleinik O, Shamaev A, Yosifian G, Mathematical Problems in Elasticity and Homogenization, 1st ed., vol. 26, North Holland; 1992.
[12] Cioranescu D, Donato P. An introduction to homogenization, Oxford lecture series in mathematics and its applications. Oxford University Press; 1999.
[13] Ramírez-Torres A, Penta R, Rodríguez-Ramos R, Merodio J, Sabina FJ, Bravo-Castillero J, Guinovart-Díaz R, Preziosi L, Grillo A. Three scales asymptotic homogenization and its application to layered hierarchical hard tissues. Int J Solids Struct 2018;130–131:190–8. https://doi.org/10.1016/j.ijsolstr.2017.09.035.
[14] Chatzigeorgiou G, Efendiev Y, Charalambakis N, Lagoudas DC. Effective thermoelastic properties of composites with periodicity in cylindrical coordinates. Int J Solids Struct 2012;49(18):2590–603. https://doi.org/10.1016/j.ijsolstr.2012.05.023.
[15] Rodríguez-Ramos R, Guinovart-Díaz R, López-Realpozo JC, Bravo-Castillero J, Otero JA, Sabina FJ, Berger H, Würkner M, Gabbert U. Micromechanical analysis of fibrous piezoelectric composites with imperfectly bonded adherence. Arch Appl Mech 2014;84(9):1565–82. https://doi.org/10.1007/s00419-014-0856-8.
[16] Berger H, Würkner M, Otero JA, Guinovart-Díaz R, Bravo-Castillero J, Rodríguez-Ramos R. Unit cell models of viscoelastic fibrous composites for numerical computation of effective properties. In: Altenbach H, Pouget J, Rousseau M, Collet B, Michelitsch T, editors. Generalized models and non-classical approaches in complex materials 1 Advanced structured materials Springer International Publishing; 2018. p. 69–82. https://doi.org/10.1007/978-3-319-72440-9_5.
[17] Li Q, Chen W, Liu S, Wang J. A novel implementation of asymptotic homogenization for viscoelastic composites with periodic microstructures. Compos Struct 2019;208:276–86. https://doi.org/10.1016/j.compstruct.2018.09.056.
[18] Hashin Z. Viscoelastic behavior of heterogeneous media. J Appl Mech 1965;32(3):630–6. https://doi.org/10.1115/1.3627270.
[19] Hashin Z. Complex moduli of viscoelastic composites-i. general theory and application to particulate composites. Int J Solids Struct 1970;6(5):539–52. https://doi.org/10.1016/0020-7683(70)90029-6.
[20] Hashin Z. Complex moduli of viscoelastic composites-ii. fiber reinforced materials. Int J Solids Struct 1970;6(6):797–807. https://doi.org/10.1016/0020-7683(70)90018-1.
[21] Mandel J. Cours de Mécanique des milieux continus. Gauthier-Villars Editeur 1966.
[22] Christensen RM. Viscoelastic properties of heterogeneous media. J Mech Phys Solids 1969;17(1):23–41. https://doi.org/10.1016/0022-5096(69)90011-8.
[23] Lahellec N, Suquet P. Effective behavior of linear viscoelastic composites: a time-integration approach. Int J Solids Struct 2007;44(2):507–29. https://doi.org/10.1016/j.ijsolstr.2006.04.038.
[24] Dutra VFP, Maghous S, Filho AC, Pacheco AR. A micromechanical approach to elastic and viscoelastic properties of fiber reinforced concrete. Cem Concr Res 2010;40(3):460–72. https://doi.org/10.1016/j.cemconres.2009.10.018.
[25] To Q-D, Nguyen S-T, Bonnet G, Vu M-N. Overall viscoelastic properties of 2d and two-phase periodic composites constituted of elliptical and rectangular heterogeneities. Eur J Mech A Solids 2017;64:186–201. https://doi.org/10.1016/j.euromechsol.2017.03.004.
[26] Tsalis D, Chatzigeorgiou G, Charalambakis N. Homogenization of structures with generalized periodicity. Compos Part B: Eng 2012;43(6):2495–512. https://doi.org/10.1016/j.compositesb.2012.01.054.
[27] Tsalis D, Baxevanis T, Chatzigeorgiou G, Charalambakis N. Homogenization of elastoplastic composites with generalized periodicity in the microstructure. Int J Plast 2013;51:161–87. https://doi.org/10.1016/j.ijplas.2013.05.006.
[28] Briane M. Three models of non periodic fibrous materials obtained by homogenization, ESAIM. Math Modell Numer Anal 1993;27(6):759–75. https://doi.org/10.1051/m2an/1993270607591.
[29] Guinovart-Sanjuán D, Rodríguez-Ramos R, Guinovart-Díaz R, Bravo-Castillero J, Sabina FJ, Merodio J, Lebon F, Dumont S, Conci A. Effective properties of regular elastic laminated shell composite. Compos Part B: Eng 2016;87:12–20. https://doi.org/10.1016/j.compositesb.2015.09.051.
[30] Taber LA. Nonlinear theory of elasticity. Applications in biomechanics. World Scientific 2004.
[31] Christensen RM. Theory of viscoelasticity – 2nd edition an introduction. Academic Press; 1982.
[32] Pipkin AC. Lectures on viscoelasticity theory. second edition Edition: Springer-Verlag; 1986.
[33] Persson L, Persson L, Svanstedt N, Wyller J. The homogenization method. An introduction; 1993.
[34] Cruz-González OL, Rodríguez-Ramos R, Otero JA, Bravo-Castillero J, Guinovart-Díaz R, Martínez-Rosado R, Sabina FJ, Dumont S, Lebon F, Sevostianov I. Viscoelastic effective properties for composites with rectangular cross-section fibers using the asymptotic homogenization method. In: Altenbach H, Pouget J, Rousseau M, Collet B, Michelitsch T, editors. Generalized models and non-classical approaches in complex materials 1. Advanced structured materials, vol. 89. Springer International Publishing; 2018. p. 203–22.
[35] Hashin Z. Theory of fiber reinforced materials, NASA contractor report. NASA CR-1974; 1972.
[36] Hanyga A, Seredyńska M. Relations between relaxation modulus and creep compliance in anisotropic linear viscoelasticity. J Elast 2007;88(1):41–61. https://doi.org/10.1007/s10659-007-9112-6.
[37] Hollenbeck K. Invlap.m: a matlab function for numerical inversion of laplace transforms by the hoog algorithm.https://www.mathworks.com/matlabcentral/answers/uploaded_files/1034/invlap.m.
[38] Srigutomo W. Gaver-stehfest algorithm for inverse laplace transform. URLwww.mathworks.com/matlabcentral/fileexchange/9987.
[39] Cavalcante MAA, Marques SPC, Pindera M-J. Transient finite-volume analysis of a graded cylindrical shell under thermal shock loading. Mech Adv Mater Struct 2011;18(1):53–67. https://doi.org/10.1080/15376494.2010.519225.
[40] Cavalcante MAA, Marques SPC. Microstructure effects in wavy-multilayers with viscoelastic phases. Eur J Mech A Solids 2017;64:178–85. https://doi.org/10.1016/j.euromechsol.2017.03.003.
[41] Liao J, Vesely I. A structural basis for the size-related mechanical properties of mitral valve chordae tendineae. J Biomech 2003;36(8):1125–33. https://doi.org/10.1016/S0021-9290(03)00109-X.
[42] Katz A, Trinh C, Wright J, Tu W, Pindera M-J. Plastic strain localization in periodic materials with wavy brick-and-mortar architectures and its effect on the homogenized response. Compos Part B: Eng 2015;68:270–80. https://doi.org/10.1016/j.compositesb.2014.08.037.
[43] Liu S, Chen KZ, Feng XA. Prediction of viscoelastic property of layered materials. Int J Solids Struct 2004;41(13):3675–88. https://doi.org/10.1016/j.ijsolstr.2004.01.015.
[44] Saravanakumar K, Farouk N, Arumugam V. Effect of fiber orientation on mode-i delamination resistance of glass/epoxy laminates incorporated with milled glass fiber fillers. Eng Fract Mech 2018;199:61–70. https://doi.org/10.1016/j.engfracmech.2018.05.027.
[45] Martynenko VG, Lvov GI. Numerical prediction of temperature dependent anisotropic viscoelastic properties of fiber reinforced composite. J Reinf Plast Compos 2017:1–12.
[46] Jochum C, Grandidier JC, Smaali M. Proposal for a long-fibre microbuckling scenario during the cure of a thermosetting matrix. Compos Part A: Appl Sci Manuf 2008;39(1):19–28. https://doi.org/10.1016/j.compositesa.2007.09.012.
[47] Otero JA, Bravo-Castillero J, Guinovart-Díaz R, Rodríguez-Ramos R, Maugin GA. Analytical expressions of effective constants for a piezoelectric composite reinforced with square cross-section fibres. Arch Mech 2003;55(4):357–71. https://doi.org/10.24423/aom.135.
[48] Guinovart-Sanjuán D, Vajravelu K, Rodríguez-Ramos R, Guinovart-Díaz R, Bravo-

Castillero J, Lebon F, Sabina FJ. Analysis of effective elastic properties for shell with complex geometrical shapes. Compos Struct 2018;203:278–85. https://doi.org/10.1016/j.compstruct.2018.07.036.
[49] Zhang J, Ostoja-Starzewski M. Mesoscale bounds in viscoelasticity of random composites. Mech Res Commun 2015;68:98–104. https://doi.org/10.1016/j.mechrescom.2015.05.005.
[50] Zhang J, Ostoja-Starzewski M. Frequency-dependent scaling from mesoscale to macroscale in viscoelastic random composites. Proc R Soc A 2016;472(2188):0801. https://doi.org/10.1098/rspa.2015.0801.
[51] Pathan MV, Tagarielli VL, Patsias S. Numerical predictions of the anisotropic viscoelastic response of uni-directional fibre composites. Compos Part A: Appl Sci Manuf 2017;93:18–32. https://doi.org/10.1016/j.compositesa.2016.10.029.